

THERMAL ANNEALING EFFECT ON UNENTANGLED STAR-SHAPED
POLYSTYRENE RESIDUAL LAYER

A Thesis

Presented to

The Graduate Faculty of The University of Akron

In Partial Fulfillment

of the Requirements for the Degree

Master of Science

Boer Liu

May, 2018

THERMAL ANNEALING EFFECT ON UNENTANGLED STAR-SHAPED
POLYSTYRENE RESIDUAL LAYER

Boer Liu

Thesis

Approved:

Accepted:

Advisor
Dr. Mark D. Foster

Dean of the College
Dr. Eric J. Amis

Faculty Reader
Dr. Mesfin Tsigie

Dean of the Graduate School
Dr. Chand Midha

Department Chair
Dr. Coleen Pugh

Date

ABSTRACT

In thin melt films of polymer chains, chains near the substrate adsorb onto the solid and form an irreversibly adsorbed layer¹. Studies show that thermal annealing is able to facilitate the adsorptions¹. To date, most studies have focused on linear-polystyrene². It should be noted that the properties of thin films of branched chains are different from the properties of films of their linear analogs³. Thus, researchers are curious regarding the adsorption of branched chains at polymer/solid interfaces. In this work, thin films of well-defined 5k and 15k star-shaped polystyrene (SPS) were thermally annealed at a temperature 60 °C above the polymer's glass transition temperature. X-ray reflectivity results reveal the thickness of the irreversibly adsorbed layer (h_{ad}) remaining after a film cooled to room temperature is immersed multiple times in toluene. For 15k SPS ($R_g \sim 2.1$ nm) that layer thickness is rapidly established as 1.5 nm ($0.7 R_g$) and remains at that value with annealing. For 5k SPS ($R_g \sim 1.2$ nm), however, h_{ad} increases to $2R_g$ after five days of annealing. Further study reveals also the chain architecture effects on the formation kinetics of the adsorbed layer. The time required for the adsorbed layer thickness to reach steady state for 5k SPS is more than one order of magnitude

larger than that for 5k LPS. This difference is attributed to a greater cooperativity required for rearrangement in the layer of star chains, even though the molecules are formally unentangled. Moreover, the thickness of the steady state adsorbed layer relative to the radius of gyration (h_{ad}/R_g) for the star polymer is 1.5 times higher than for the linear polymer.

ACKNOWLEDGEMENTS

I would like to express my deepest appreciation to my advisor Professor Mark D. Foster for his expert advice, useful remarks, and enormous encouragement throughout my research. I would like to thank Professor Mesfin Tsigie for his patient during my thesis preparation and tremendous inspiration of study star-shaped macromolecules.

I am especially grateful to Dr. Qiming He, former group member in Prof. Foster's group for his kindly help and invaluable assistance.

I would like to express my gratitude to all my group members in Prof. Foster's research group for their help and discussions.

Finally, I would like to express to thank my beloved parents for their infinite supports.

TABLE OF CONTENT

LIST OF FIGURES	ix
LIST OF TABLES	xii
CHAPTER	
I. INTRODUCTION.....	1
II. BACKGROUND.....	4
2.1 Thin films of star-shaped polymers.....	4
2.1.1 Bulk properties of star-shaped polymers	4
2.1.2 Anomalous properties in confined star-shaped polymer films	5
2.2 The adsorbed layer at the polymer and substrate interface	8
2.3 Experimental techniques	15
2.3.1 Spin coating	15
2.3.2 Annealing.....	16
2.4 Characterization methods	17
2.4.1 Ellipsometry.....	17
2.4.2 Atomic force microscopy (AFM).....	18

2.4.3 X-ray reflectivity(XR)	20
III. EXPERIMENTAL.....	24
3.1 Materials.....	24
3.2 Sample preparation.....	25
3.3 Characterization techniques for studying film thickness and surface morphology	26
3.3.1 Ellipsometry.....	26
3.3.2 Atomic force microscope (AFM)	27
3.3.3 X-ray reflectivity (XR)	28
IV. RESULTS AND DISCUSSION.....	29
4.1 Effect of annealing on the irreversibly adsorbed layer of 15k and 5k SPS. 29	
4.1.1 Thickness of the adsorbed layer (h_{ad}).....	29
4.1.2 Surface morphology of the irriversibly adsorbed layer of SPS	39
4.2 Comparison of effect of annealing on h_{ad} between linear and star PS of same molecular weight	45

V. CONCLUSION.....	49
REFERENCES	52

LIST OF FIGURES

Figure	Page
1. Schematic structures of the polystyrene chains in this study.....	3
2. Diagram of the difference between the T_g of the film and the T_g of the bulk, ΔT_g ($T_{g, \text{film}} - T_{g, \text{bulk}}$) for SPS thin films. Reprinted with permission from Glynos, et al. ¹⁵ Copyright 2015 American Chemical Society	6
3. Comparison of viscosities obtained from XPCS data (open symbols) with viscosities from bulk rheology (filled symbols) as a function of $T - T_{g, \text{bulk}}$ for branched architectures as marked. Reprinted figure with permission from Wang, S.-f.; Foster, M. D., <i>Physical Review Letters</i> 2013 , <i>111</i> (6), 068303. Copyright 2014 by the American Physical Society	7
4. Schematic view of the two different chain conformations in the adsorbed layer. Reprinted with permission from Gin <i>et al.</i> ²⁸ © 2012 American Physical Society, used with permission.....	9
5. Kinetics of irreversible adsorption of (a) PS thin films on SiO ₂ , Reprinted with permission from Housmans, et al. ³¹ © 2014 American Chemical Society, used with permission and (b) PS ($M_w = 290\text{kDa}$), PMMA ($M_w = 97\text{kDa}$), and P2VP ($M_w = 200\text{kDa}$), on H-Si, from Jiang, et al. ⁷ © 2014 American Chemical Society, used with permission.	11
6. Schematic illustrations of adsorbed layers of thin films of (a) 6kDa cyclic (left) and linear PS (right) (Reprinted with permission © 2016 American Chemical Society) ⁵ . (b) Linear PS ($M_w = 131\text{ kDa}$) on H-Si (left) and on a plasma polymerized film (right) according to Zhou <i>et al.</i> ³⁴ © 2017 American Chemical Society.....	14

7. Stages of spin coating using static dispensing of the solution. Copyright of Ossila Ltd 2014, used with permission. https://www.ossila.com/pages/spin-coating	16
8. Geometry of an ellipsometry experiment, showing the s- and p- directions. Copyright J.A. Woollam Company, Used with Permission.	18
9. Force-distance curve for AFM. Reproduced with permission. © 2017 Nanoscience Instruments	19
10. Scheme of an X-ray beam reflected and refracted at a planar, sharp interface	21
11. (a) Calculated reflectivity curves versus scattering angle 2θ from silicon against air for an X-ray wavelength of 1.54 \AA or surface roughness (rms) of 0.5 nm and 2 nm or a constant background assumed to be equivalent to $R = 10^{-7}$. (b) Reflectivity curves of Au film Si substrates with different film thickness. Again, a constant background of 10^{-7} has been added to the calculated reflectivity. Copyright © 2017 — Rigaku Corporation and its Global Subsidiaries. Used with permission.	23
12. Thickness of the irreversibly adsorbed layer of (a) 15k SPS and (b) 5k SPS films versus annealing time.....	31
13. XR curves and their corresponding fits for (a) 15k SPS and (c) 5k SPS irreversibly adsorbed layer. The corresponding profiles of SLD against distance from the polymer/air interface are shown in (b) and (d). The SLD profiles are offset for clarity by $2.5 \times 10^{-6} \text{ \AA}^{-2}$ at the SLD axis for clarity. The dashed vertical lines	

correspond to the centers of interfaces in the original box models that were convoluted with interface profiles to create the overall SLD profile..... 37

14. AFM height images ($1\ \mu\text{m} \times 1\ \mu\text{m}$) of the (a) 1 h, (b) 24 h, (c) 42 h, and (d) 70 h irreversibly adsorbed layers of 15k SPS. The average roughness (RMS) is 0.55 ± 0.03 nm. (e) The height profile along the white line in (d) obtained using Section Analysis in NanoScope Analysis..... 40

15. AFM height images ($1\ \mu\text{m} \times 1\ \mu\text{m}$) of the (a) 0.2 h, (b) 24 h, (c) 48 h, and (d) 108 h irreversibly adsorbed layers of 5k SPS. The average roughness (RMS) is 0.45 ± 0.05 nm. (e) The height profiles along the line cuts in (d) were obtained using Section Analysis in NanoScope Analysis..... 41

16. (a) AFM height image of 24 h bottom layer and (b) the height profile along the white line obtained using Section Analysis in NanoScope Analysis. The scan size and the height scale in (a) are $1\ \mu\text{m} \times 1\ \mu\text{m}$ and -2 to 2 nm. 44

17. The value of h_{ad} relative to R_g of 5k SPS (left axis) and LPS (right axis) as a function of annealing time. 47

LIST OF TABLES

Table	Page
1. Characteristics of the polymers in the study	24
2. Parameter values for film structure models used to construct SLD profiles for fits to the XR data for 15k SPS.....	38
3. Parameter values for film structure models used to construct SLD profiles for fits to the XR data for 5k SPS.....	38

CHAPTER I

INTRODUCTION

Thin films are used in a vast array of industrial applications for which wetting, friction, and adhesion of these films are important. To meet various industrial demands, the thicknesses of thin films have been decreased to the value comparable to the size of polymer chains. Fundamental physical and chemical properties of thin films, including their structures, chain conformations, and dynamics, vary substantially from those of the bulk. The phenomena of properties changing with decreasing film thickness belong to a family of behavior known as “confinement effects”⁴. Confinement effects show distinctions when it comes to polymer films composed of chains having different architectures. Thin melt films of branched chain have slow surface dynamics compared with those of the films of linear chains¹. It should be noted that when polymer films are sufficiently thin, the system cannot be considered as homogeneous⁵. For a supported thin film, the dynamical inhomogeneity can be roughly described using a three-layer model. The layer at the very top of the film, at the free surface will in general have different dynamics than the rest of the film. The middle layer may have bulk-like properties

if the film is thick enough. An “immobile layer,” which has a viscosity that may be considered to be infinite is next to the substrate. There is growing attention to this bottom immobile layer, which is sometimes referred to as the “adsorbed layer”. Finer distinctions among these various terms will be clarified later. Evidence has been found that dynamical confinement effects ⁶ and segmental relaxations ⁷ depend strongly on this immobile layer. The morphology ⁸, formation ⁸, stability ⁹, and adhesion properties ¹⁰ of the adsorbed layer of entangled linear polystyrenes have quite recently been extensively studied.

This thesis starts with consideration of the simplest branched chain, SPS (Figure 1) of two molecular weights and describes characterization of the adsorbed layer using different techniques from various aspects. There has been work showing that the adsorbed layer of the SPS is very important in stabilizing the whole thin films ¹¹. Simulation results have also captured that the star molecules packed densely near the solid Substrate However, little has been done on the direct observation of the adsorbed layer for star-branched chain. The work described reveals the morphology of the adsorbed layer and the formation kinetics of this layer.



Figure 1. Schematic structures of the polystyrene chains in this study.

CHAPTER II

BACKGROUND

2.1 Thin films of star-shaped polymers

2.1.1 Bulk properties of star-shaped polymers

A star-shaped polymer is a branched polymer with linear chains (the arms) radiating from a central branching point (the core). Because of their unique structures, star polymers can be tailored¹² and used as additives to modify and control the properties of materials¹³. The first synthesized star-shaped polymer was a polyamide reported by John Schaeffgen and Paul Flory in 1948¹⁴.

The star molecule's behavior varies in with the combination of functionality (arm number), f and arm length, N . With increasing f and decreasing N , the star adopts a core-corona structure¹¹. The combination of star structure and size brings star polymers distinct properties compared with those of their linear analogs. One of the properties is bulk viscosity¹⁵. When below the critical molecular weight for entanglement, melts of a branched polymer can have a bulk viscosity much lower than that of its linear analog. However, the viscosity of a melt of an entangled branched polymer can be several orders of magnitude larger than that of its linear analog.

2.1.2 Anomalous properties in confined star-shaped polymer films

In ultrathin films, polymer chains are confined by two interfaces. Experiments and simulations have shown that the films thickness dependent T_g ¹⁶⁻¹⁷, dynamic fragility¹⁸⁻¹⁹, viscosity²⁰, and local density²¹ in both supported films and free-standing films. It is widely believed that at polymer/air interfaces, the presence of the free surface results in higher chain mobilities⁴ in the case of linear chains, while substrate effects result in the reduction of mobilities at polymer/substrate interfaces²². Glynos *et al.* extensively studied the thin films of SPS ranging from $f=2$ to 64 and values of chain arm length, M_w^{arm} , from 4 to 140 kg/mole. In the study of T_g ¹⁶, a transition has been found from film T_g lower than the bulk T_g , to film T_g higher than bulk T_g , as shown in Figure 2. This transition occurred with increasing f or decreasing N wherein f appears to be the stronger effect. The same group reported that compared to the linear polymers, star PS materials has lower aging rates²³ and better wetting²⁴. These imply that thin films of star polymers are more stable over the time and can be considered as an alternation material of thin films of linear polymers.

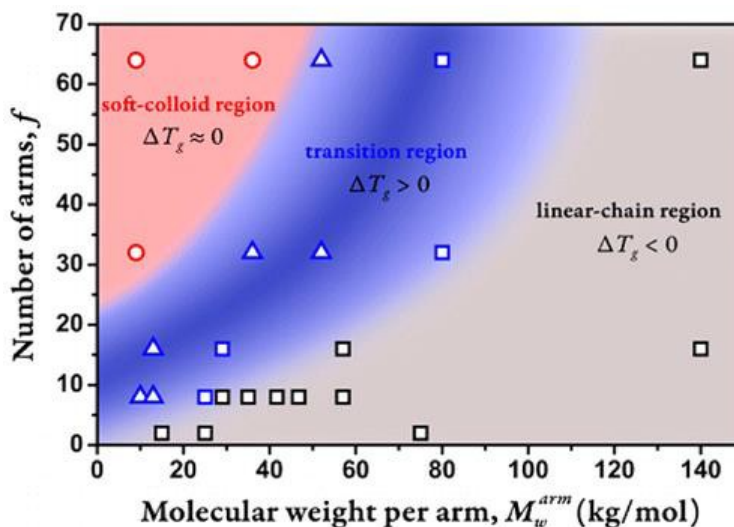


Figure 2. Diagram of the difference between the T_g of the film and the T_g of the bulk, ΔT_g ($T_{g, \text{film}} - T_{g, \text{bulk}}$) for SPS thin films. Reprinted with permission from Glynos, et al.¹⁶ Copyright 2015 American Chemical Society.

Previous works in Foster's group studied the dependence of thin films surface fluctuation on different molecular architectures. Introduction or elimination of branches significantly alters the melt surface fluctuations¹. The viscosities inferred from XPCS (η_{XPCS}) for linear chains over a wide range of film thicknesses coincide with values for bulk viscosity (η_{Bulk}). However, for branched PS the values of η_{XPCS} for films about $20 R_g$ thick can be as much as two orders of magnitude higher than η_{Bulk} , as shown in Figure 3. Moreover, more densely branched comb PSs show smaller values of ($\eta_{XPCS} - \eta_{Bulk}$) than do less densely branched PSs. The

authors conjectured that is because the more compact polymers have less penetrable volume, and thus hinder the movement of neighboring molecules less.

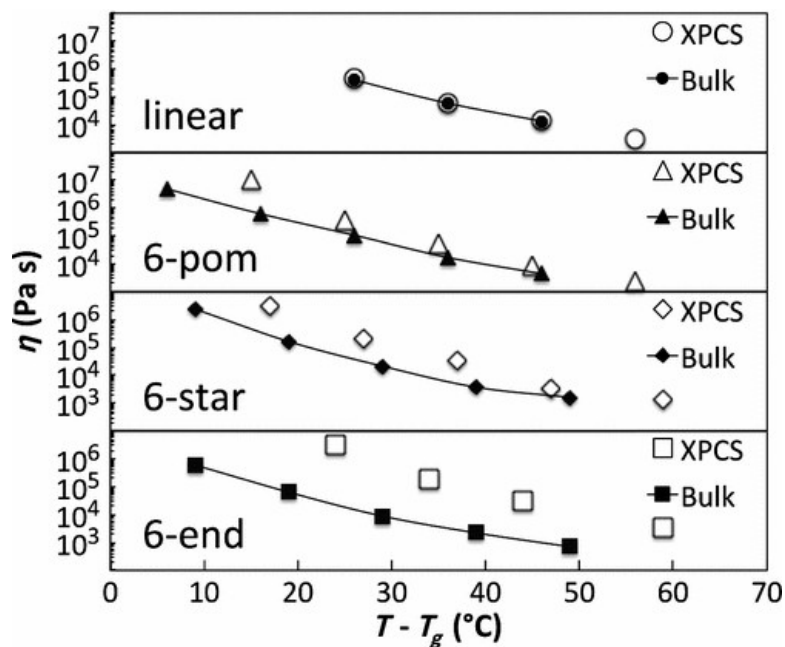


Figure 3. Comparison of viscosities obtained from XPCS data (open symbols) with viscosities from bulk rheology (filled symbols) as a function of $T - T_{g,bulk}$ for branched architectures as marked. Reprinted figure with permission from Wang, S.-f.; Foster, M. D., *Physical Review Letters* **2013**, *111* (6), 068303. Copyright 2014 by the American Physical Society.

2.2 The adsorbed layer at the polymer and substrate interface

When polymer chains from a solution are gathered at an interface in a condensed layer, we say that the polymer has “adsorbed” to the interface. Polymer adsorption to solid surfaces from solution has been studied extensively. For a polymer solution next to a substrate, whether adsorption will occur depends on the net adsorption energy of the polymer segment. For adsorption to occur the difference between the segment/surface contact free energy and the solvent/surface contact free energy must be negative²⁵. In other words, the energy of the system is lowered when a polymer segment takes the place of a solvent molecule on the solid surface. Guiselin’s approach²⁶ suggested for revealing the adsorbed layer at the interface can be used for both adsorption from solution and adsorption from the melt: by immersing or rinsing the thin films with a good solvent. The unadsorbed chains are pulled away from the films. E. Jenkel and B. Rumbach first proposed adsorbed molecule structures schematically²⁷. These consisted of “trains”, which are parts of the chains directly in contact with the substrate; “loops”, which connect with two trains and have no contact with the substrate surface; and “tails”, which contain non-adsorbing segments, and extend away from the substrate. Granick and co-workers²⁸ developed a picture of this process of polymer adsorbing on the solid

based on this model. Molecules which first arrive adsorb onto the surface, leaving a little spacing for the later-arriving molecules to adsorb. In the case of pure polymer melts, Koga *et al.* proposed the formation mechanism of a layer strongly adsorbed on the substrate from the melt ²⁹ shown in Figure 4. The molecules arriving first form a dense “flattened layer”. The late arriving ones adsorb at points in the open spaces to form a loosely adsorbed layer. The “flattened layer” and the “loosely adsorbed layer together compose the immobile layer, also known as the interfacial layer.

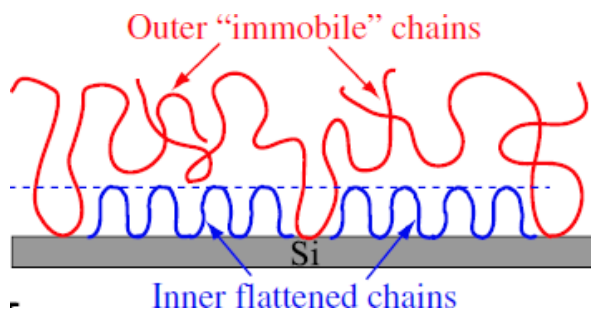


Figure 4. Schematic view of the two different chain conformations in the adsorbed layer. Reprinted with permission from Gin *et al.* ²⁹ © 2012 American Physical Society, used with permission.

The study of the adsorbed layer from melt films has received lots of attention.

Durning and coworkers ³⁰ found h_{ad} of poly (methyl methacrylate) (PMMA) on

quartz is scaled as $N^{0.47 \pm 0.05}$, N is the degree of polymerization. Tsui and coworkers³¹ found h_{ad} of polystyrene(PS) on H-Si and SiO₂ increases as annealing. Moreover, h_{ad} of polystyrene(PS) on H-Si is higher than that on SiO₂. Thermal annealing is one of the ways to accelerate the adsorption of the chains onto the solid. It has been found that the thickness of the adsorbed layer builds up as thin films are annealed^{8, 32}. Napolitano and coworkers³² found that the formation kinetics of the adsorbed layer has two regimes, a power law growth regime and a later linear growth regime until h_{ad} reaches to a steady state. The two regimes are separated by a crossover time t_{cross} , as shown in Figure 5 (a). According to the experiment and the simulation, the adsorption rate increases with increasing temperature, T , while the film thickness, h , or the adsorption amount is T independent. Further study of the mechanism of the adsorption³³ reveals that the thermal energy only affects the adsorption rate, while the interfacial interaction determines the adsorbed amount. In another study of the formation kinetics of the adsorbed layer on a H-Si substrate, the power law growth with a crossover, t_{cross} , is found in the films of entangled PS, PMMA, and poly (2-vinyl pyridine) (P2VP), as shown in Figure 5 (b).

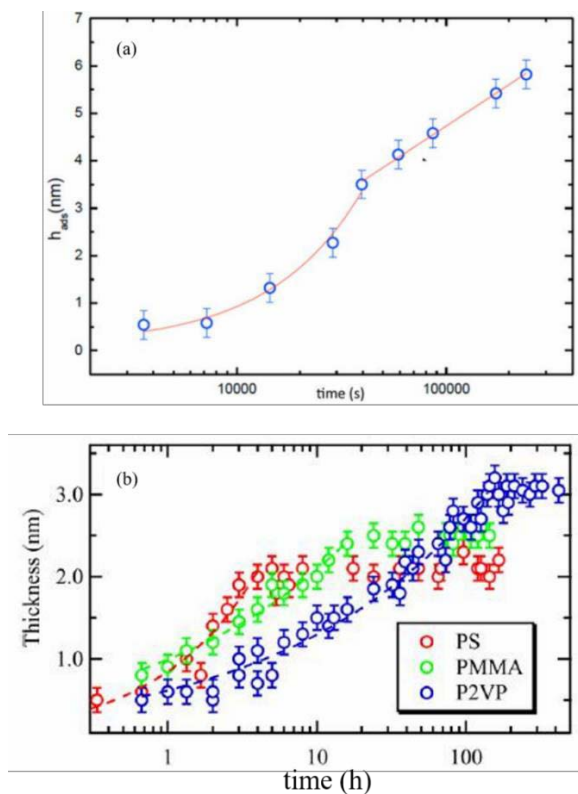


Figure 5. Kinetics of irreversible adsorption of (a) PS thin films on SiO₂, Reprinted with permission from Housmans, et al. ³² © 2014 American Chemical Society, used with permission and (b) PS ($M_w = 290\text{kDa}$), PMMA ($M_w = 97\text{kDa}$), and P2VP ($M_w = 200\text{kDa}$), on H-Si, from Jiang, et al. ⁸ © 2014 American Chemical Society, used with permission.

It has been over 20 years since confinement effects in polymer thin films were found ¹⁷. Recently researchers have shifted the attention from the polymer/air interface to the polymer/solid interface. Ongoing work is revealing the connection

between the macroscopic properties and the presence of the adsorbed layer at polymer/solid interface. A recent study³⁴ demonstrates that the T_g in thin films of poly(4-tert-butylstyrene) is reduced as thickness is decreased. However, the formation of the adsorbed layer can cancel the free surface effect and cause the T_g to recover to a value comparable to that of the bulk through prolonged annealing. An enhanced segmental movement is found in poly (4-chloro styrene) thin films with dielectric spectroscopy. The recovery of the α -relaxation is related to the development of the adsorbed layer through annealing⁷.

When the thickness of the film is sufficiently small, dynamical confinement of cyclic PS thin films can be observed using XPCS⁶. The adsorbed layer of the cyclic PS films has been determined to be higher than that of their linear analog films, as shown in Figure 6 (a). When the thickness of the film is decreased to 16 times the estimated chain radius of gyration (R_g), the effect of the adsorbed layer shows up, resulting in slowing down of the surface movement of cyclic PS thin films, whereas no confinement effect is found for the linear PS films with similar thickness or even for thickness of $7 R_g$. In another study³⁵, substrate chemistry is modified using deposition of a thin coating using plasma polymerization³³ to create a plasma polymerized film (pp-film). After modification, there is no adsorbed layer observed

on the pp-films after rinsing with toluene. However, there still is some slowing of the surface fluctuations when the film is in the melt. There must be an adsorbed layer at the time the XPCS measurements are done, even though that adsorbed layer on the pp-layer does not survive rinsing with toluene. The authors argue that the adsorbed layer on the pp-film is smaller than that on silicon. Because of the thinner adsorbed layer, shown in Figure 6 (b), the surface fluctuations of PS on the pp-film are less susceptible to the decrease of thickness compared to those of PS on H-Si.

These studies are in agreement with what has been found in thin films in which chains have been intentionally tethered to the substrate by covalent bonds, rather than by physisorption. For example, if a PS brush is formed³⁶ by means of tethering all the PS chains on a substrate, a thin film surface can be realized for which all fluctuations are so slow that they are outside the measurement window for the XPCS instrument. However, even more similar to the case of physisorption is the case of films in which only a portion of the PS chains are covalently tethered to the substrate. Such films were studied by Lee *et al*³⁷. They differ from the melt films with physisorbed chains only in the fact that the tethered chains are tethered at just one end, rather than at multiple points of physisorption.

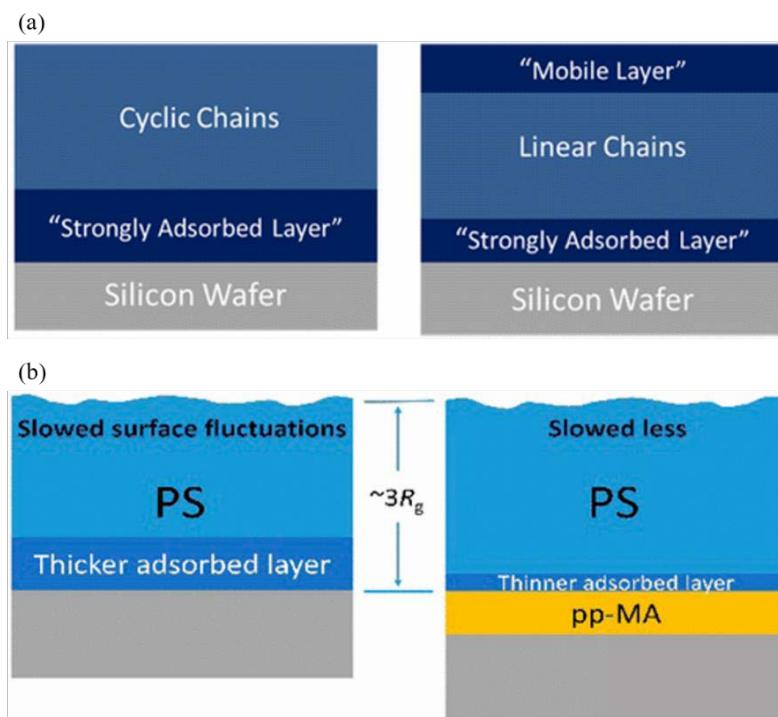


Figure 6. Schematic illustrations of adsorbed layers of thin films of (a) 6kDa cyclic (left) and linear PS (right) (Reprinted with permission © 2016 American Chemical Society)⁶. (b) Linear PS ($M_w = 131$ kDa) on H-Si (left) and on a plasma polymerized film (right) according to Zhou *et al.*³⁵ © 2017 American Chemical Society.

So much is known about the formation of adsorbed layers in the case of linear film. Researchers studied the formation, morphology, and thickness of the adsorbed layer and how whole film properties affected by this layer. The linear polymers studied have different molecular chemistries and M ranging from several kDa to hundreds of kDa. However, little has been addressed from the perspective of chain

architectures. There are remaining questions for adsorbed layers of SPS. For example, are the kinetics of adsorption the same as for linear polymers? Are the layers formed of the same thickness as for linear chains? Are the adsorbed layers composed of two layers? Are these layers of the same morphologies as for linear chains? In this work, unentangled 4 arm SPS are considered to study the adsorbed layers of star polymers. X-ray Reflectivity (XR), Atom Force Microscopy (AFM), and ellipsometry are used to answer the questions listed above.

2.3 Experimental techniques

2.3.1 Spin coating

Spin coating is one of the most widely used techniques for applying a thin film to a substrate. The thin film thicknesses are well controlled and determined by tuning solvent concentration and spinning speed. The spin coating process can be divided into four stages: (1) Firstly, solution is deposited onto the substrate. (2) The substrate rotates at high speed and the majority of the solution is flung off the substrate. (3) The solvent evaporates rapidly as air flows above the film. (4) Lastly, the film dries to leave the polymer on the substrate in an even covering.

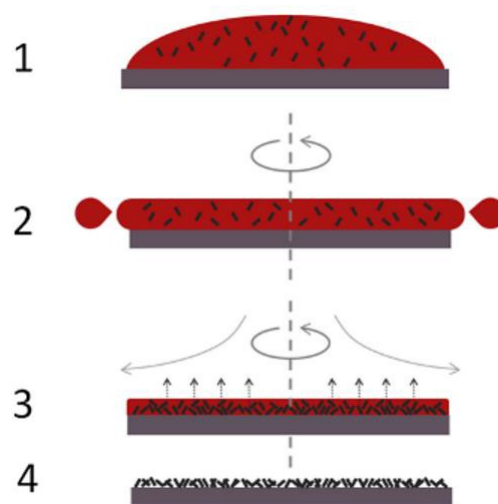


Figure 7. Stages of spin coating using static dispensing of the solution. Copyright of Ossila Ltd 2014, used with permission. <https://www.ossila.com/pages/spin-coating>

In fact, the solvent cannot fully evaporate, resulting in a small amount being trapped in the cast film due to the fast evaporation process³⁸. Furthermore, this rapid solvent evaporation process leads to nonequilibrium conformations of polymer chains. Both disadvantages can be alleviated through thermal annealing.

2.3.2 Annealing

Annealing is a thermal treatment in which polymer chains can eliminate the residual stress and retained solvent caused by spin coating. Prolonged thermal

annealing is typically required for fully relaxing the polymer chains and expediting polymer adsorption from melt to solid ³⁹. In 1993, Satija and coworkers ⁴⁰ observed the negative expansion of an ultrathin film while heating using X-ray reflectivity. Later, Kanaya and coworkers ⁴¹ found that this abnormal phenomenon is due to an unrelaxed structure, that is, lack of annealing of thin films.

2.4 Characterization methods

2.4.1 Ellipsometry

Ellipsometry is a versatile optical technique used for thin film characterization. As shown in the Figure 8, an ellipsometer includes all the following: light source, polarization generator, sample, polarization analyzer, and detector. The incident polarized beam undergoes amplitude and phase changes of the s- and p- components when reflected. Ellipsometry expresses these two changes by measuring two values: Ψ and Δ . The first parameter $\Psi=|R_p|/|R_s|$ refers to the ratio of reflection coefficients for the parallel and perpendicular components. The second parameter is given by $\Delta=\delta_{in}-\delta_{out}$, where δ_{in} is the phase difference between s- and p- component of the incoming wave and δ_{out} is that of the outgoing wave. By developing a model in the software using known parameters and fitting the model

to the measured data, the thickness and reflective index of the thin film can be obtained.

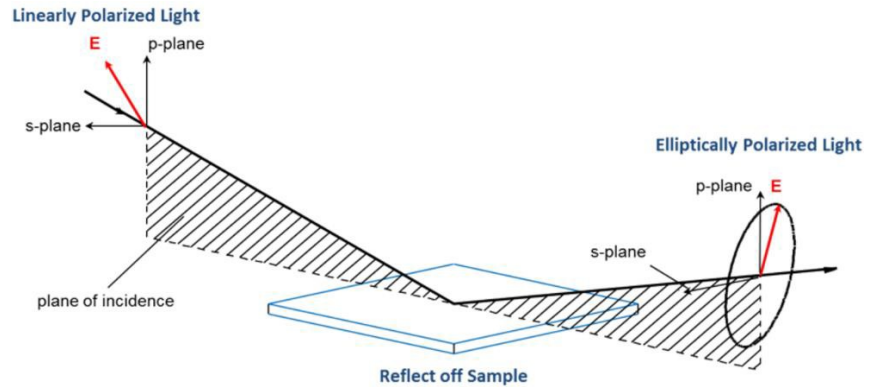


Figure 8. Geometry of an ellipsometry experiment, showing the s- and p-directions. Copyright J.A. Woollam Company, Used with Permission.

2.4.2 Atomic force microscopy (AFM)

The scanning probe microscopy (SPM) is a technique used to physically study the surface at an atomic scale level. The first SPM was scanning tunneling microscopy (STM) developed by IBM Zurich in 1988⁴². STM uses a tunneling current of electrons between the sample and tip to probe the surface image, which means the surface of the sample must be conductive. This limitation of STM drove the invention of AFM, one kind of SPM. Like STM, AFM maps the surface with a

sharp tip. The tip is a couple of microns height and 8 -10 nm in diameter. The tip is located at the end of a micron-long cantilever with a low spring constant. The forces due to van der Waals and other forces between the sample surface and tip cause the cantilever to bend and bring the tip close to surface. Whether the interaction is attractive or repulsive forces depends on the distance between the sample and tip, as shown in figure below.

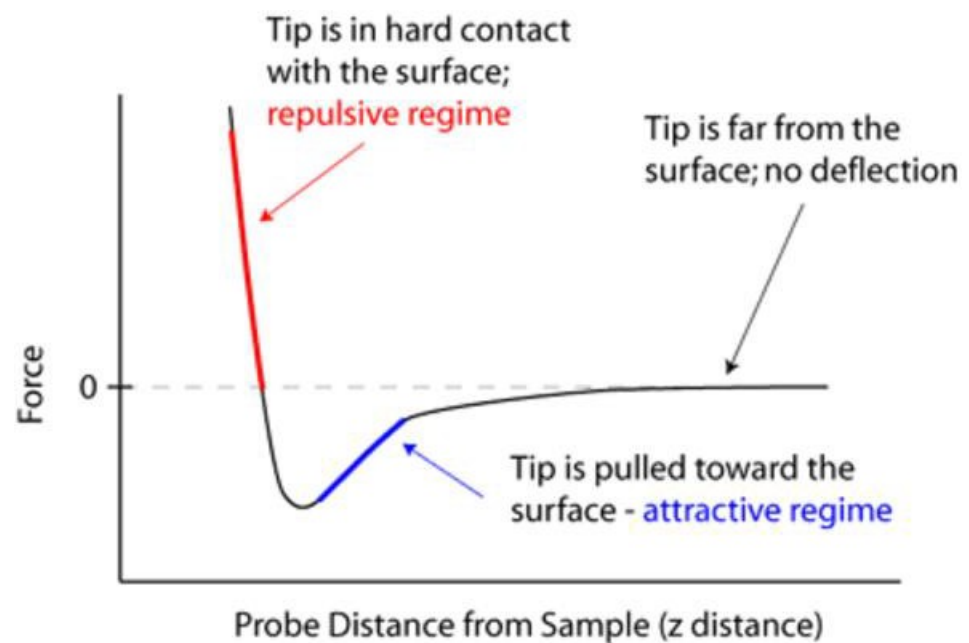


Figure 9. Force-distance curve for AFM. Reproduced with permission. © 2017 Nanoscience Instruments.

Two regimes are labeled in Figure 9, the repulsive regime and attractive regime. Contact mode imaging is performed in the repulsive regime. The cantilever is held less than a few angstroms from the sample surface whereas in non-contact mode imaging, which is performed in the attractive regime the tip tens to hundreds of angstroms above the surface. In tapping mode⁴³ imaging, a stiff cantilever vibrates above the sample surface, and the amplitude of vibration changes in response to changes in the spacing between the average tip position and sample surface. In the intermittent contact (tapping) regime⁴⁴, the AFM tip constantly contacts the surface and lift the tip. In this way, the AFM tip and sample surface are both damaged less easily than in contact mode, and, at the same time, AFM can achieve high resolution.

2.4.3 X-ray reflectivity(XR)

XR is a long-established technique widely utilized for thin film study. Surface and interface roughness, film thickness, and density can be determined with X-ray reflectivity in a nondestructive manner if there is enough contrast among different layers in the film. In the specular reflection geometry, as shown in Figure 10, the angle with respect to the surface at which the beam is reflected, θ equals the incident angle, θ_0 . X-rays undergo total external reflection if θ_0 is smaller than the critical

angle, θ_c , which is specific to the medium 1. For θ_0 above this angle, the incident beam begins to penetrate the sample, and a substantial part of the incident beam is refracted, while a part of the incident beam is reflected. The intensity of the reflected beam depends on the angle θ_0 and the contrast between medium 0 and medium 1. This contrast can be expressed in terms of the refractive indices of the two media, n_0 and n_1 . The angle of refraction can be calculated using Snell's equation:

$$n_0 \cos \theta_0 = n_1 \cos \theta_1. \quad (1)$$

When $\theta_1 = 0$:

$$n_0 \cos \theta_c = n_1. \quad (2)$$

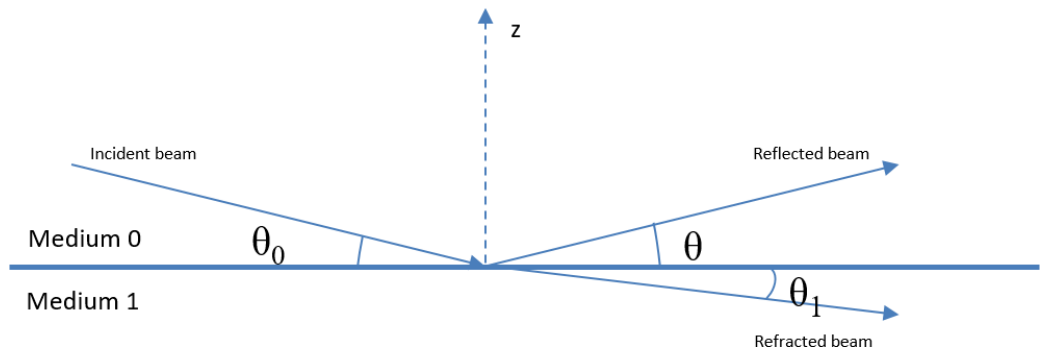


Figure 10. Scheme of an X-ray beam reflected and refracted at a planar, sharp interface.

When X-rays impinge on an ideally smooth surface of a semi-infinite medium of uniform refractive index, *e.g.* silicon surface with air, the reflectivity curve decreases monotonically for θ_0 beyond θ_c . For θ_0 below θ_c , reflectivity, R (the reflected intensity, I , relative to incident intensity, I_0 , or I_0 / I) remains unity (if absorption is ignored). As θ_0 increases beyond θ_c , R decreases rapidly. The reflectivity curve decays more rapidly if the roughness of the interface increases (as shown in Figure 10 (a))⁴⁵. The reflectivity curve will no longer be monotonic if the sample has a structure more complicated than that of single uniform medium. A typical reflectivity curve for a uniform single layer on a substrate has the following features: (1) A sharp drop in R at the $2\theta_c$. (2) The envelope of the curve decays monotonically with increasing incident angle. (3) Oscillations in R with incident angle, known as “Kiessig fringes”⁴⁶ appear. The fringes appear due to the interference among the X-rays reflected from the air-film and film-substrate interfaces.

X-ray reflectivity curves for films with different thicknesses on a Si substrate are shown in Figure 10 (b)⁴⁵. Film thickness has an inverse relation with fringe spacing, *i.e.*, larger fringe spacing corresponds to a thicker film. Although it

requires fitting to obtain the precise value of the film thickness, one can estimate the film thickness from the fringe spacing:

$$h \approx 2\pi/\Delta q, \quad (3)$$

Where h is the estimated film thickness and Δq is the difference between the values of scattering vector for successive maxima or minima in the reflectivity curve.

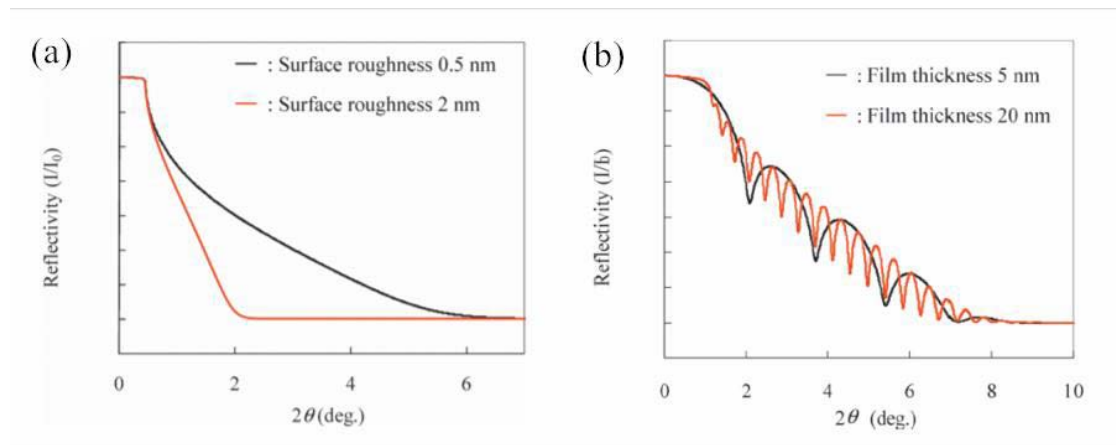


Figure 11. (a) Calculated reflectivity curves versus scattering angle 2θ from silicon against air for an X-ray wavelength of 1.54 \AA or surface roughness (rms) of 0.5 nm and 2 nm or a constant background assumed to be equivalent to $R = 10^{-7}$. (b) Reflectivity curves of Au film Si substrates with different film thickness. Again, a constant background of 10^{-7} has been added to the calculated reflectivity. Copyright © 2017 — Rigaku Corporation and its Global Subsidiaries. Used with permission.

CHAPTER III

EXPERIMENTAL

3.1 Materials

Linear polystyrene (LPS) was purchased from Scientific Polymer Products Inc. and used as-received. Monodisperse SPS were synthesized using anionic polymerization and a silicon-chloride linking reaction⁴⁷⁻⁵⁰. The number-average molecular weight (M_n), polydispersity (PDI), and bulk glass transition temperatures ($T_{g, bulk}$) are listed in Table 3.1.

Table 1. Characteristics of the polymers in the study.

Materials	M_n^a (g/mol)	PDI	$T_{g, bulk}^b$ (°C)
LPS5	5000	1.02	85 ⁵¹
4SPS5	5100 ^a	1.06 ^a	69.0 ⁵²
4SPS15	14900 ^a	1.04 ^a	88 ^b

^a By size exclusion chromatography coupled with refractive index detection ($\pm 5\%$) in THF at 30 °C.

^b Determined by DSC with heating rate 10 °C/ min.

3.2 Sample preparation

LPS and SPS solutions in toluene (Fisher Chemical, ACS), each with concentration of 1.5 wt% were prepared and the polymer allowed to dissolve overnight. The solutions were filtered (0.45 μ m, Restek, PTFE) at least six times before sample preparations. Polished silicon wafers (EL-CAT Inc.) were cut into 1.5cm x 2cm pieces. Firstly, silicon wafers were rinsed with deionized water and dried with nitrogen several times to clean the surfaces. Wafer pieces were further cleaned in a hot piranha solution (up to 120 °C)⁵³, a 3:1 mixture of concentrated sulfuric acid (H₂SO₄) and hydrogen peroxide (H₂O₂), for at least 20 min. Then, the wafer pieces were rinsed with pure water. Wafers were submerged in 50 ml 1% hydrofluoric acid (HF) (Aelf Aesar, ACS) aqueous solution for 40 seconds to remove the native oxide layer and rinsed with water subsequently. Lastly, the polymer solution was spun cast (spin speed = 2000 rpm) on the etched silicon pieces. It should be noted that the wafer was spun immediately after HF etching and pure water rinsing. The films were annealed in a high vacuum (ca. 1 x 10⁻⁷ Pa) oven and quenched (ca. 200 °C/min quench rate) to room temperature in vacuum. The average heating rate was 3 °C/min. The annealing time was counted as soon as the

temperature reached the target temperature (within 0.1 °C).

To reveal the morphology, thickness, and density of the strongly adsorbed layer, the annealed samples were treated using Guiselin's approach²⁶ executed using the protocol developed by Dr. Koga and co-workers²⁹. A film was immersed in 100 ml toluene for 10 min and then dried with nitrogen. Then, the sample was put back to the toluene used before. This immersion and drying was repeated five times. Last, the sample was put in high vacuum oven at room temperature overnight. The layer which remains after the rinsing is the irreversibly adsorbed layer.

3.3 Characterization techniques for studying film thickness and surface morphology

3.3.1 Ellipsometry

Measurements with a spectroscopic ellipsometer (M-2000, J.A. Woollam) were used to determine the thickness of the immobile layer. The refractive index varies with polymer and wavelength. For a typical sample of polystyrene, the visible light refractive index (RI) is 1.589 at a wavelength of 638 nm. Thicknesses were estimated by fitting the data using a constant RI (1.589). This means the thickness values are subject to some error, depending on how much the densities of

the adsorbed layers varied among chains of different architectures and films annealed for different times. He *et al.*⁴⁸ found that the density of the adsorbed layer for linear chains was only 80% of the density for bulk chains, while the density for the adsorbed layer of cyclic chains was about 98% of that for bulk chains. Thickness measurements with XR are generally more precise, but the XR instrument was not available for some portion of the time over which the measurements were made.

3.3.2 Atomic force microscope (AFM)

Surface morphologies of films of LPS and SPS were studied using a Veeco Dimension Icon AFM from Bruker Inc. The AFM was operated in tapping mode under ambient condition. Commercial n-type silicon probes with a cantilever length of 12-18 μm and tip size of 8 nm (μmasch , HQ: NSC35/Cr-Au BS) were chosen for the measurements. The spring constant of the cantilever was 5.4-16 N/m and the resonant frequency was typically 300 kHz. The scan rate was 1.0 Hz with scanning density of 512 lines per frame. Height images and phase images were acquired simultaneously.

3.3.3 X-ray reflectivity (XR)

The detailed adsorbed layer structures were revealed using XR. The XR measurements were done on a home-built reflectometer on an 18-kW rotating anode (RA-HF18, Rigaku) with CuK_α radiation ($\lambda = 1.54 \text{ \AA}$). The wavelength and angle divergences were 0.005 \AA and $2 \times 10^{-6} - 3 \times 10^{-4}$. The XR curves were fitted using MOTOFIT with a two-layer model (Si substrate and a polymer layer).

CHAPTER IV

RESULTS AND DISCUSSION

4.1 Effect of annealing on the irreversibly adsorbed layer of 15k and 5k SPS

4.1.1 Thickness of the adsorbed layer (h_{ad})

To begin, it would be useful to describe the terminology used here to refer to samples. The designation “xx hours + irreversibly adsorbed layer” means a spin-coated film annealed for xx hours, then treated using the Guiselin approach, and finally dried in high vacuum at room temperature overnight. For example, “1 h irreversibly adsorbed layer” refers to a SPS spin-coated film annealed for 1 h, then treated with the Guiselin approach and finally dried in the vacuum. The annealing time ranged from 0.2 h to 108 h. The annealing temperature were set to be 60 °C above T_g . The thickness of the irreversibly adsorbed layer is plotted against the annealing time in Figure 11. These thicknesses were determined from XR measurements. For 15k SPS, as shown in Figure 11 (a), h_{ad} remains constant within the uncertainty at 1.45 ± 0.06 nm or about $0.69 R_g$., from the smallest time measured through 70 h. According to simulations by Koutsos *et al.*⁵⁴ of a single star polymer with low functionality (f) adsorbing from solution, the chain adopts

highly aspherical conformations on the surface to which it adsorbs. Especially for 4-arm star polymers, the arms spread out from the cores and the molecules adsorb like a plate on the plane⁵⁴. According to these simulations, the height of an adsorbed molecule should be comparable to the backbone size. However, the value of h_{ad} observed is about twice the backbone size of PS chains (0.8 nm)⁵⁵. This seems reasonable, since, in the pure polymer melt film, molecules adsorbing to the substrate cannot spread out as readily as a single molecule adsorbing in the solution simulation. Rather, the arms of one adsorbed star are likely to penetrate into the pervaded volumes of neighboring adsorbed chains and lie on top of arms of these neighboring chains cover others. Therefore, the resulting h_{ad} is higher than the backbone size due to the overlapping of parts of adjacent molecules.

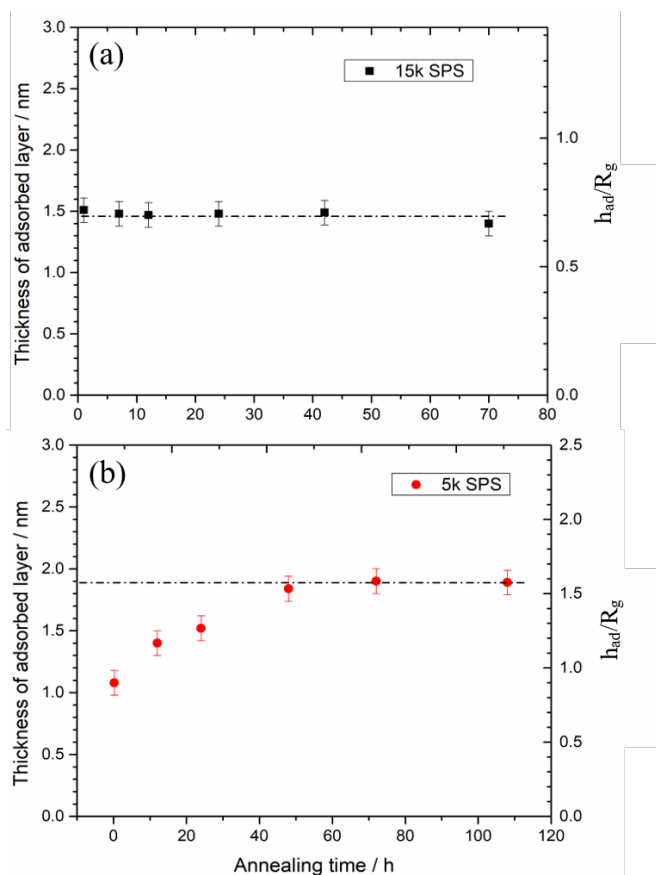


Figure 12. Thickness of the irreversibly adsorbed layer of (a) 15k SPS and (b) 5k SPS films versus annealing time.

The effects of the annealing on h_{ad} of 5k SPS are strikingly different. As shown in Figure 11 (b), h_{ad} increases from 1.1 ± 0.1 nm to 1.9 ± 0.1 nm, or from $0.97 R_g$ to $1.55 R_g$, in 50 hours. According to recent work of Napolitano *et al.*³³, the final adsorbed amount of for linear polymers is determined by the strength of the polymer/substrate interaction potential, and therefore does not vary much with

temperature. Also, they maintain that the equilibrium adsorbed amount is not dictated by the molecular motions of rearrangement. However, linear polymers of higher M do build thicker adsorbed layers. In contrast, the value of h_{ad} for 5k SPS is substantially larger than that for the 15k SPS in terms of both absolute thickness and thickness relative to R_g . So, the star chains behave dramatically differently than the linear chains behave.

There are two remarkable features of the behavior to be explained. The first is that no change in adsorbed amount with annealing time is observed for the larger star, while for the smaller one there is a definite transition from an initial absorption behavior to saturation. The second is the fact that the equilibrium adsorbed amount (both in absolute sense and relative to R_g) is larger for the smaller star. First, we consider the development in adsorbed amount with time. It appears that adsorbed 5k SPS chains can rearrange easily. M_{arm} of 5k SPS is far below the critical molecular weight for entanglement. 5k SPS is small, and since the arms are quite short and relatively stiff, there may be a lower tendency for 5k SPS chains to “get in each other’s way” when absorbing on the surface. Also, after the segments of 5k SPS molecules adsorb onto a surface, the chains may be more likely to rearrange. The current picture for adsorption of linear chains ³² is that rearrangement becomes

less frequent as the thermal annealing progresses and as opportunities to further optimize the organization of the adsorbed chains are exhausted. It would seem that this should be true for 5k SPS also. According to our study, it takes 50 hours for the 5k SPS chains to rearrange and reach the steady state.

As far as the 15k SPS goes, it appears very few rearrangements can occur after the initial adsorption, or if they do occur they do little to change the thickness. We propose that this is because the arms are long enough to interpenetrate with each other and the star architecture allows for ways of one chain stuck to the surface to constrain another chain that simply are not possible with linear chains. This confines the movement of the 15k SPS molecules, resulting in few changes of adsorbed conformations after the initial adsorption of the star.

The second feature to be explained is the larger adsorbed amount, h_{ad} , for the smaller star. This may also be due to the fact that the 5k SPS can rearrange more readily, in the sense that the 5k SPS adsorbed layer can more readily optimize its structure. However, in order to build this thicker layer clearly more than one layer of 5k SPS molecules must be involved. If the chains can readily rearrange, how does a second layer of 5k SPS chains get trapped or “stuck” at the surface of the substrate? We do not yet have an answer for this, but may obtain some additional

insight by characterizing the structure of the adsorbed layers further with XR and AFM.

XR curves for the irreversibly adsorbed layers of both types of star molecules are plotted in Figure 13a and 12c. The solid lines correspond to best fits to the XR curves. The best fit was obtained using a model containing two media (from bottom to top: a Si substrate and a PS layer); the best fit parameters used can be found in

Table 2 and Table 3. It is apparent by inspection of the data that the adsorbed layer for 15k SPS does not change much with annealing time while the adsorbed layer for 5k SPS changes quite a bit. The weak minima in the curves for the 15k SPS layers indicate some sort of thin layer is present, but may not be very well defined.

Figure 13 (b) shows the SLD depth profiles of the adsorbed layers for 15k

SPS. These show that the polymer material reflecting the X-rays in each case is not in the form of a well-defined layer. The “thickness” of adsorbed layer reported above for the 15k SPS films capture an apparent thickness corresponding to the distance over which the SLD increases nearly linearly from 5.1 to $16.0 \times 10^{-6} \text{ \AA}^{-2}$. The nominal values of scattering length density (SLD) are $10 \times 10^{-6} \text{ \AA}^{-2}$ for the “boxes” used to represent the polymer layer in the film structure models before convolution with interface profiles for both 15k and 5k SPS, 10% higher than the SLD of the bulk SPS films ($9.1 \times 10^{-6} \text{ \AA}^{-2}$). The nominal thickness reported is that corresponding to the region between the two vertical dotted lines superposed on the SLD plots. These vertical lines mark the centers for the air/polymer interface and polymer/substrate interface convolution functions used to construct the SLD profile to fit the XR data.

It must be noted that the SLD does not capture three dimensional details of the layer structure. The SLD profile corresponds to a one-dimensional projection of the structure onto the z-axis. Nonetheless, it is possible to say that near the substrate, the polymer chains are densely packed because the SLD there is on the order of the SLD of bulk PS chains (ca. $9.1 \times 10^{-6} \text{ \AA}^{-2}$). Near the air, the polymer segments are less densely distributed and the SLD varies nearly linearly through

the layer. The linear change of SLD has been created using a model of the layer in which the sum of the roughnesses of the two interfaces (air/polymer and polymer/substrate) is comparable to the apparent thickness of the layer, as may be seen from the model parameter values listed in

Table 2. However, XR cannot distinguish if the layer structure actually has two sharp, rough interfaces so that the laterally averaged SLD corresponds to such a 1-D SLD profile or whether everywhere in the film the density actually varies gradually from the substrate surface to the air interface. Rather, one can only conclude that the adsorbed layer extends about 1.5 nm up from the substrate. Making the distinction between a layer with rough interfaces and a smooth layer with a gradient in SLD with depth everywhere in the film would require off-specular scattering measurements or AFM imaging (see below).

In Figure 13 (c), there is a noticeable change in the shape of XR curve with annealing time. The inset shows the corresponding SLD profile along the depth.

The profile of 0.2 h and 24 h adsorbed layers of 5k SPS has the similar gradient with that of 15k SPS, shown in Figure 13 (d). As the annealing progresses, the SLD of the adsorbed layer becomes more defined. Ultimately, there is a well-defined SLD for the adsorbed layer at 108 h, determined to be $10.0 \times 10^{-6} \text{ \AA}^{-2}$.

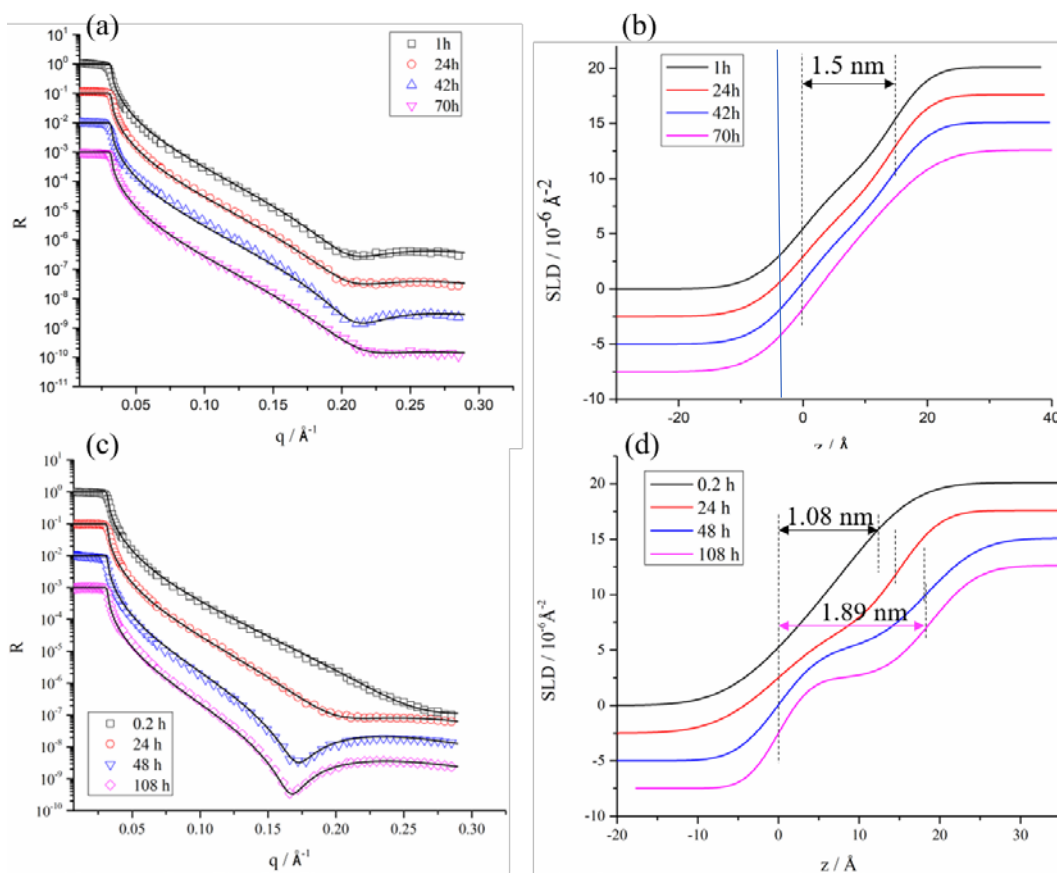


Figure 13. XR curves and their corresponding fits for (a) 15k SPS and (c) 5k SPS irreversibly adsorbed layer. The corresponding profiles of SLD against distance from the polymer/air interface are shown in (b) and (d). The SLD profiles are offset for clarity by $2.5 \times 10^{-6} \text{ \AA}^{-2}$ at the SLD axis for clarity. The dashed vertical

lines correspond to the centers of interfaces in the original box models that were convoluted with interface profiles to create the overall SLD profile.

Table 2. Parameter values for film structure models used to construct SLD profiles for fits to the XR data for 15k SPS

t / h	h_{ad} / nm	SLD / $\times 10^{-6} \text{ \AA}^{-2}$	$\sigma_{SPS/air}$ / nm	$\sigma_{SPS/substrate}$ / nm
1	1.51	10.0	0.62	0.51
24	1.48	10.0	0.65	0.52
42	1.49	10.1	0.61	0.56
70	1.40	10.2	0.69	0.63

Table 3. Parameter values for film structure models used to construct SLD profiles for fits to the XR data for 5k SPS

t / h	h_{ad} / nm	SLD / $\times 10^{-6} \text{ \AA}^{-2}$	$\sigma_{SPS/air}$ / nm	$\sigma_{SPS/substrate}$ / nm
0.2	1.08	9.9	0.62	0.57
24	1.52	10.0	0.63	0.40
48	1.84	10.0	0.41	0.52
108	1.89	10.0	0.32	0.45

4.1.2 Surface morphology of the irreversibly adsorbed layer of SPS

The AFM height images of the adsorbed layers at each annealing time for 15k SPS are shown in Figure 14 (a)-(d). The surface of the irreversibly adsorbed layer of the 15k SPS has a “blob-like” structure on it. The average diameter can be calculated using NanoScope Analysis. The average diameters of the “blob” are determined to be 16nm, 18 nm, 17 nm, 16nm, for (a)-(e). Figure 14 (e) gives the height profile along the white line along the surface diagonally across the image in (d) for the 70 h irreversibly adsorbed layer. The spikes correspond to the outlines of the “blobs” on the surface. In the Figure 15, the surfaces of the 5k SPS irreversibly adsorbed layers are seen to have similar textures, but with a lower areal density of blobs.

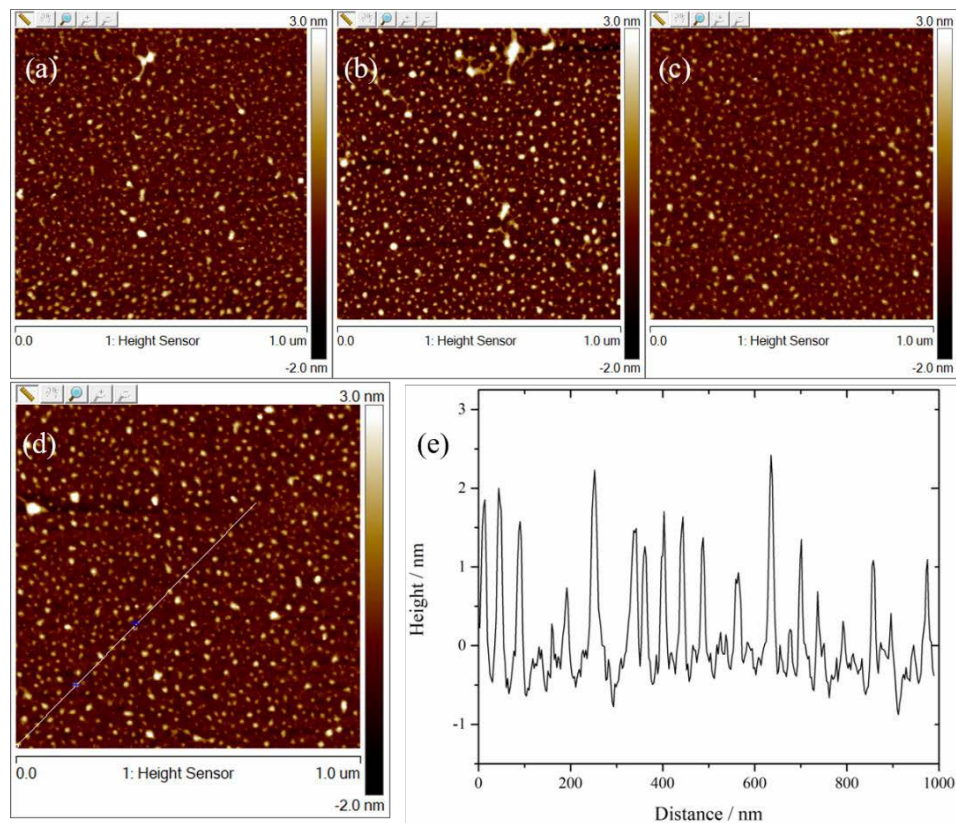


Figure 14. AFM height images ($1 \mu\text{m} \times 1 \mu\text{m}$) of the (a) 1 h, (b) 24 h, (c) 42 h, and (d) 70 h irreversibly adsorbed layers of 15k SPS. The average roughness (RMS) is $0.55 \pm 0.03 \text{ nm}$. (e) The height profile along the white line in (d) obtained using Section Analysis in NanoScope Analysis.

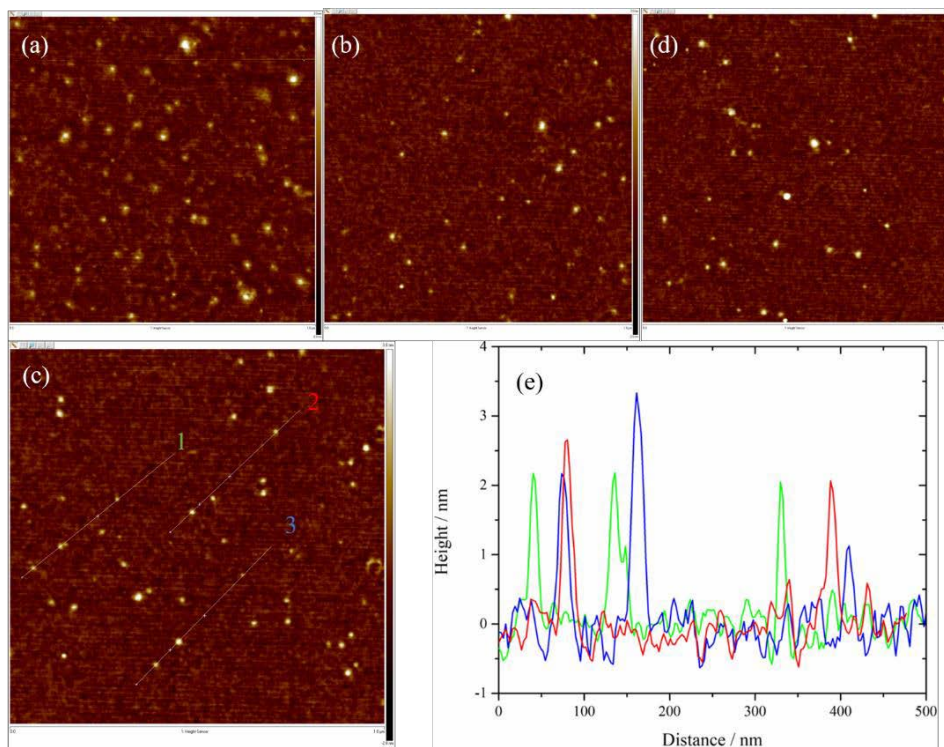


Figure 15. AFM height images ($1 \mu\text{m} \times 1 \mu\text{m}$) of the (a) 0.2 h, (b) 24 h, (c) 48 h, and (d) 108 h irreversibly adsorbed layers of 5k SPS. The average roughness (RMS) is $0.45 \pm 0.05 \text{ nm}$. (e) The height profiles along the line cuts in (d) were obtained using Section Analysis in NanoScope Analysis.

Koga *et al.* studied the irreversibly adsorbed layer of films of linear polymers with molecular weight M_n . When M_n was higher than 50k, the adsorbed layer was composed of a bottom strongly adsorbed layer and an adjacent loosely adsorbed layer⁹. The adsorbed layer was obtained by rinsing the film in toluene. The surface of the adsorbed layer was smooth. Then, the adsorbed layer was treated with

chloroform and the loosely adsorbed chains aggressively pulled away from the substrate, leaving a “flattened layer” on the substrate. An “island” feature has been found using AFM ⁸. However, for molecules of M_n smaller than 50k, there was only a bottom layer (flattened layer) in the film ². The formation of the outer layer required the chains to be long enough to fold and be pinned in vacant spaces of the flattened layer, as shown in Figure 4. In the case of M_n below 50k, the chains are too short to form the outer layer.

The surface of the adsorbed layer obtained after chloroform immersion for 15k SPS film in this study is shown in Figure 16 (a). The AFM image shows a “ridges and holes” structure on the surface. Though the surface morphology after the immersion with the more aggressive solvent (chloroform) is different from the surface morphology after immersion with toluene, the adsorbed layer of 15k SPS molecules is not likely composed of two layers. Rather, it seems that in a single layer the star molecules are adsorbed more or less strongly. Molecules with more segment attaching points adsorb more tightly to the surface, thus requiring stronger solvents to be pulled away. Molecules with few attaching points adsorb loosely onto the substrate. Here, toluene takes the unadsorbed chains away from the film. Chloroform, with a stronger ability to solvate PS, takes away the loosely adsorbed

molecules. The leaving of these molecules left the vacant spaces seen as “holes” in the image in Figure 16 (a). However, this change in the 3-D morphology of the film has the effect of decreasing slightly the value of h_{ad} derived from XR. To study further the way in which removing chains impacted the layers, they were examined using ellipsometry before and after chloroform immersion. The value of h_{ad} determined from ellipsometry by keeping the refractive index constant in the fitting dropped from 3.0 nm to 2.3 nm. However, the AFM imaging suggests the true difference in h_{ad} was smaller than 0.7 nm. The RI used to fit the data was the RI of the bulk value. Because of the presence of the holes, the value of h_{ad} (after chloroform immersion) assigned in this way has to be lower than the true h_{ad} . In order to further look at the changes of the thickness, the height profile along the white lines in Figure 14 (d) and Figure 16 (a) are plotted in Figure 14 (e) and Figure 16 (b). The peak to valley heights for both profiles are 2.5-3 nm suggesting the actual change in h_{ad} is much less than 0.7 nm. So, we come back to the idea that the adsorbed layer of the SPS is not really composed of two layers, but rather one layer with some loosely adsorbed chains embedded in it and these more loosely adsorbed chains get pulled out by the chloroform. The differences in behavior between the adsorbed layers of star PS and the adsorbed layers of linear chains suggest something interesting about

the ability of star chains below entanglement molecular weight to interpenetrate. In a manner similar to linear chains with M below 50k these small stars do not build a complete “second layer” that has a smooth surface and resists toluene removal. However, for stars the flattened layer is still able to hold onto some stars that stick up above the flattened layer, but cannot be removed with toluene. With stronger solvent, such as chloroform, these stars that had been sitting in holes in the flattened layer are taken away leaving the holes in Figure 16 (a).

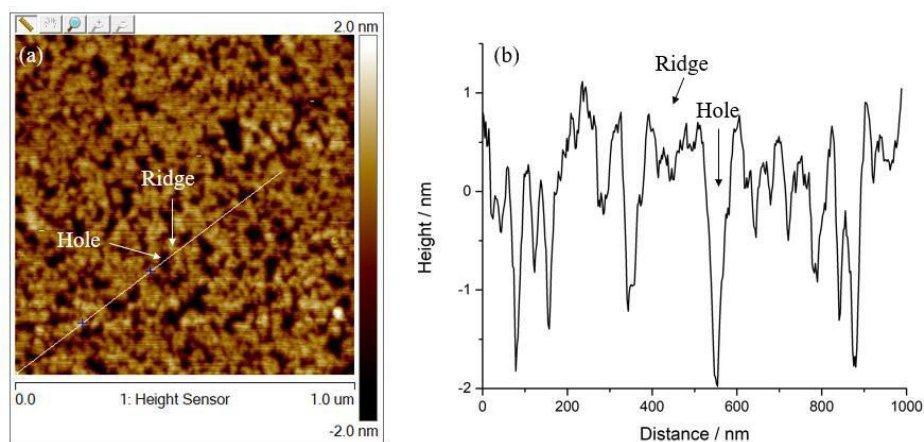


Figure 16. (a) AFM height image of 24 h bottom layer and (b) the height profile along the white line obtained using Section Analysis in NanoScope Analysis. The scan size and the height scale in (a) are $1 \mu\text{m} \times 1 \mu\text{m}$ and -2 to 2 nm.

4.2 Comparison of effect of annealing on h_{ad} between linear and star PS of same molecular weight

It has been examined how M affects the formation of the adsorbed layer for four arm star chains. Though general comparison with the behavior of linear chains of various molecular weights has been made the comparison for architecture effects was made more precisely by considering matched analogs and also the comparison was focused on M_n far from entanglement. Thin films of 5k SPS and LPS were prepared using spin coating, annealed at $T = 60$ °C above T_g), and treated using the Guiselin approach. Then, h_{ad} was determined using ellipsometry. The ellipsometric parameters Ψ and Δ were fitted using a Cauchy model⁵⁶ with bulk values (1.589). Figure 17 plots a normalized adsorbed layer thickness h_{ad}/R_g against annealing time for both star and linear. The value of $h_{ad, 4SPS5}$ increases from $2.0 R_g$ to $2.9 R_g$ and that for $h_{ad, LPS5}$ from $0.9 R_g$ to $1.2 R_g$. Here it is noticed that the value of thickness determined from ellipsometry and XR are not comparable. This is because the values of RI and thickness are highly coupled in the analysis of the ellipsometry data, whereas they are practically decoupled in the XR analysis. Even so, the ellipsometry data are enough to reveal differences in trends between the $h_{ad, 4SPS5}$ and $h_{ad, LPS5}$ values. The first observation is that $h_{ad, 4SPS5}$ at steady state is higher

than the steady state value for $h_{ad, LPS5}$. In a star molecule, the arms of the star are tethered to a core. The conformations of an arm next to the core are highly hindered. At these regions, the arms are stretched to compensate steric-hindrance effects. The stretching leads to a reduction in the number of chain conformations for a star in the bulk as compared to linear chain of the same M_n in the bulk. When star molecules are drawn close to a substrate, there is a lower reduction of conformational entropy per chain and therefore less entropy penalty in the chain free energy than for the case of the linear analog. The adsorption of star molecules to a substrate is thus slightly more favorable than is the adsorption of linear analogs to the same surface. Given sufficient time, then, to optimize the adsorbed layer structure, a higher adsorbed layer thickness results for the star melt than for the linear melt.

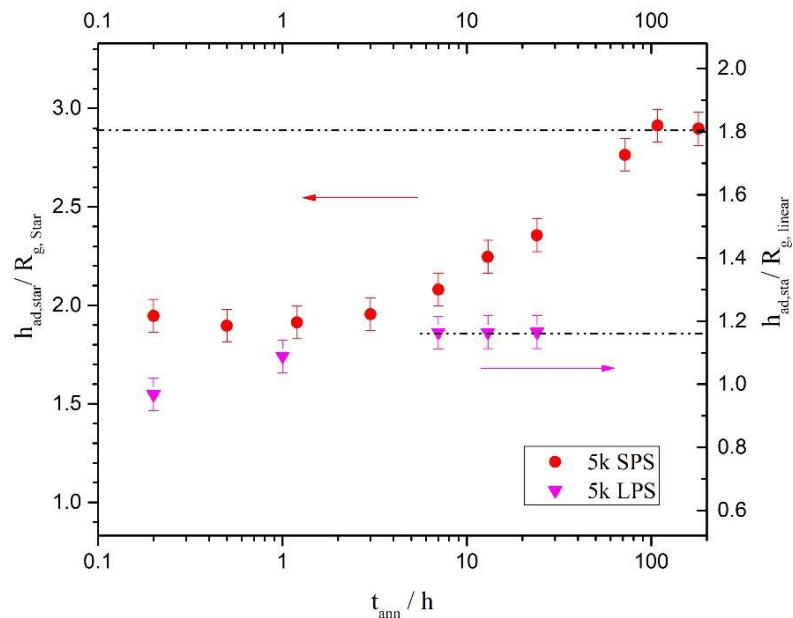


Figure 17. The value of h_{ad} relative to R_g of 5k SPS (left axis) and LPS (right axis) as a function of annealing time.

Another observation is that the time required to reach the steady state value of adsorbed layer thickness is more than 10 times longer for the star chains. It takes 100 hours for $h_{ad, 4SPS5}$ to reach the steady state value, whereas it takes 8 hours or less for $h_{ad, LPS5}$ to reach its steady state value. It appears that the motions of star chains that allow the structure of the adsorbed layer to optimize are much slower than the motions key to optimizing the adsorbed layer of linear chains. The linear chain layer is already changing thickness at 1 hour annealing time, but the star layer

thickness does not begin to increase until about 7 hours of annealing. Perhaps those motions for the star chain are slower because they involve coordinated movements of multiple arms or ends, while the linear chains can move toward optimum with the movement of only one chain end.

CHAPTER V

CONCLUSIONS

In this research, we investigated the evolution of the irreversibly adsorbed layer of four-arm SPS with annealing and characterized h_{ad} , layer density and layer surface morphology using multiple techniques. First, differences between the behaviors of SPS of two molecular weights, 5k and 15k were elucidated. Secondly, differences between the evolution of adsorbed layers with annealing time for the four-arm star and linear chains of the same molecular weight, 5k were quantified.

For 5k SPS, XR measurements reveal that h_{ad} at steady state is 1.9 ± 0.1 nm ($1.6 R_g$), which is 20% higher in absolute thickness than the steady value, 1.5 nm ($0.7 R_g$), for the much larger 15k SPS. If one considers the thickness relative to R_g , the difference is 270%. This contrasts with the case of linear chains for which adsorbed layer thickness grows with molecular weight for molecular weights at which the linear chains are unentangled to consistently attain thicknesses of order R_g .⁸

The kinetics of adsorbed layer development with annealing also differ in a surprising way with molecular weight. It takes 50 h for the smaller star layer to

reach steady state, while it takes less than 1 h in for the bigger star layer to do so. Our explanation builds on the contention of by Napolitano *et al.*³³ that the formation of the adsorbed layer of SPS depends on two factors, the potential of adsorption, and rearrangement of the molecules after adsorption. The smaller stars manage to rearrange as thermal annealing goes, but this rearrangement takes many hours. However, in the case of the 15k, although M is below M_c , the arms seem already to be long enough that the chains become trapped in the layer structure formed very soon after absorbing. Comparison of the AFM with XR data suggest that the 15k SPS cannot form a second well-formed adsorbed layer atop flattened chains, but there are blobs of polymer sticking above the nominal surface which are removed by immersion in the strong solvent chloroform. The treatment yanks out of the adsorbed layer less strongly adsorbed chains that are apparently in the blobs, leaves holes in a layer having an otherwise more or less flat surface.

Lastly, the change in the evolution of the adsorbed layer with annealing time with chain architecture was studied in a controlled way using linear and star analogs of the same molecular weight. The adsorbed layer of 5k SPS is found to be thicker than that of 5k LPS, consistent with what has been found in other works²⁴. The process of forming the adsorbed layer is found to be slower for the star than for its

linear analog. This may be due to the cooperativity required to rearrange the molecules that have more chain ends. Even though they are not entangled in a conventional sense, the way in which the stars are interpenetrated, even for short arms, markedly slows the rearrangement. Although there are remaining questions, the observations made here emphasize that changing chain architecture can be used to alter the thickness, morphology, and formation rate of the very thin adsorbed layer at the polymer/solid interface that has been seen to influence glass transition behavior and surface fluctuations. There may be opportunities to exploit this control over dynamics of thin films in potential applications for industry.

REFERENCES

- (1) Wang, S.-f.; Yang, S.; Lee, J.; Akgun, B.; Wu, D. T.; Foster, M. D., Anomalous surface relaxations of branched-polymer melts. *Physical Review Letters* **2013**, *111* (6), 068303.
- (2) Sen, M.; Jiang, N.; Cheung, J.; Endoh, M. K.; Koga, T.; Kawaguchi, D.; Tanaka, K., Flattening process of polymer chains irreversibly adsorbed on a solid. *ACS Macro Letters* **2016**, *5* (4), 504-508.
- (3) He, Q.; Wang, S.-F.; Hu, R.; Akgun, B.; Tormey, C.; Peri, S.; Wu, D. T.; Foster, M. D., Evidence and Limits of Universal Topological Surface Segregation of Cyclic Polymers. *Physical review letters* **2017**, *118* (16), 167801.
- (4) Forrest, J.; Dalnoki-Veress, K.; Dutcher, J., Interface and chain confinement effects on the glass transition temperature of thin polymer films. *Physical Review E* **1997**, *56* (5), 5705.
- (5) Bernazzani, P.; Sanchez, R. F.; Woodward, M.; Williams, S., Determination of the glass transition temperature of thin unsupported polystyrene films using interference fringes. *Thin Solid Films* **2008**, *516* (21), 7947-7951.
- (6) He, Q.; Narayanan, S.; Wu, D. T.; Foster, M. D., Confinement effects with molten thin cyclic polystyrene films. *ACS Macro Letters* **2016**, *5* (9), 999-1003.
- (7) Panagopoulou, A.; Napolitano, S., Irreversible Adsorption Governs the Equilibration of Thin Polymer Films. *Physical Review Letters* **2017**, *119* (9), 097801.

- (8) Jiang, N.; Shang, J.; Di, X.; Endoh, M. K.; Koga, T., Formation mechanism of high-density, flattened polymer nanolayers adsorbed on planar solids. *Macromolecules* **2014**, *47* (8), 2682-2689.
- (9) Jiang, N.; Cheung, J.; Guo, Y.; Endoh, M. K.; Koga, T.; Yuan, G.; Satija, S. K., Stability of Adsorbed Polystyrene Nanolayers on Silicon Substrates. *Macromolecular Chemistry and Physics* **2018**, 219 (3).
- (10) Jiang, N.; Sen, M. K.; Zeng, W.; Chen, Z.; Cheung, J.; Morimitsu, Y.; Endoh, M. K.; Koga, T.; Fukuto, M.; Yuan, G., Structure-induced switching of interpolymer adhesion at a solid-polymer melt interface. *Soft Matter* **2018**.
- (11) Daoud, M.; Cotton, J., Star shaped polymers: a model for the conformation and its concentration dependence. *Journal de Physique* **1982**, *43* (3), 531-538.
- (12) Qiu, L. Y.; Bae, Y. H., Polymer architecture and drug delivery. *Pharmaceutical Research* **2006**, *23* (1), 1-30.
- (13) Kumar, S. K.; Benicewicz, B. C.; Vaia, R. A.; Winey, K. I., 50th anniversary perspective: are polymer nanocomposites practical for applications? *Macromolecules* **2017**, *50* (3), 714-731.
- (14) Schaeffgen, J. R.; Flory, P. J., Synthesis of multichain polymers and investigation of their viscosities1. *Journal of the American Chemical Society* **1948**, *70* (8), 2709-2718.
- (15) Fetters, L. J.; Kiss, A. D.; Pearson, D. S.; Quack, G. F.; Vitus, F. J., Rheological behavior of star-shaped polymers. *Macromolecules* **1993**, *26* (4), 647-654.
- (16) Glynos, E.; Frieberg, B.; Chremos, A.; Sakellariou, G.; Gidley, D. W.; Green,

P. F., Vitrification of thin polymer films: from linear chain to soft colloid-like behavior. *Macromolecules* **2015**, *48* (7), 2305-2312.

(17) Keddie, J. L.; Jones, R. A.; Cory, R. A., Size-dependent depression of the glass transition temperature in polymer films. *EPL (Europhysics Letters)* **1994**, *27* (1), 59.

(18) Zhang, C.; Priestley, R. D., Fragility and glass transition temperature of polymer confined under isobaric and isochoric conditions. *Soft Matter* **2013**, *9* (29), 7076-7085.

(19) Mansfield, K. F.; Theodorou, D. N., Molecular dynamics simulation of a glassy polymer surface. *Macromolecules* **1991**, *24* (23), 6283-6294.

(20) Masson, J.-L.; Green, P. F., Viscosity of entangled polystyrene thin film melts: Film thickness dependence. *Physical Review E* **2002**, *65* (3), 031806.

(21) Yang, Z.; Fujii, Y.; Lee, F. K.; Lam, C.-H.; Tsui, O. K., Glass transition dynamics and surface layer mobility in unentangled polystyrene films. *Science* **2010**, *328* (5986), 1676-1679.

(22) Erber, M.; Tress, M.; Mapesa, E. U.; Serghei, A.; Eichhorn, K.-J.; Voit, B.; Kremer, F., Glassy dynamics and glass transition in thin polymer layers of PMMA deposited on different substrates. *Macromolecules* **2010**, *43* (18), 7729-7733.

(23) Frieberg, B.; Glynos, E.; Sakellariou, G.; Green, P. F., Physical aging of star-shaped macromolecules. *ACS Macro Letters* **2012**, *1* (5), 636-640.

(24) Glynos, E.; Frieberg, B.; Green, P. F., Wetting of a multiarm star-shaped molecule. *Physical Review Letters* **2011**, *107* (11), 118303.

(25) Flerer, G.; Stuart, M. C.; Scheutjens, J.; Cosgrove, T.; Vincent, B., *Polymers at Interfaces*. Springer Science & Business Media: 1993.

(26) Guiselin, O., Irreversible adsorption of a concentrated polymer solution. *EPL (Europhysics Letters)* **1992**, *17* (3), 225.

(27) Jenckel, E.; Rumbach, B., Adsorption of high polymers from solution. *z. Elektrochem* **1951**, *55*, 612-618.

(28) Johnson, H. E.; Granick, S., New mechanism of nonequilibrium polymer adsorption. *Science* **1992**, *255* (5047), 966-968.

(29) Gin, P.; Jiang, N.; Liang, C.; Taniguchi, T.; Akgun, B.; Satija, S. K.; Endoh, M. K.; Koga, T., Revealed architectures of adsorbed polymer chains at solid-polymer melt interfaces. *Physical Review Letters* **2012**, *109* (26), 265501.

(30) Durning, C.; O'Shaughnessy, B.; Sawhney, U.; Nguyen, D.; Majewski, J.; Smith, G., Adsorption of poly (methyl methacrylate) melts on quartz. *Macromolecules* **1999**, *32* (20), 6772-6781.

(31) Fujii, Y.; Yang, Z.; Leach, J.; Atarashi, H.; Tanaka, K.; Tsui, O. K., Affinity of polystyrene films to hydrogen-passivated silicon and its relevance to the T_g of the films. *Macromolecules* **2009**, *42* (19), 7418-7422.

(32) Housmans, C.; Sferrazza, M.; Napolitano, S., Kinetics of irreversible chain adsorption. *Macromolecules* **2014**, *47* (10), 3390-3393.

(33) Simavilla, D. N.; Huang, W.; Vandestruck, P.; Ryckaert, J.-P.; Sferrazza, M.; Napolitano, S., Mechanisms of Polymer Adsorption onto Solid Substrates. *ACS Macro Letters* **2017**, *6* (9), 975-979.

(34) Perez-de-Eulate, N. G.; Sferrazza, M.; Cangialosi, D.; Napolitano, S., Irreversible Adsorption Erases the Free Surface Effect on the T_g of Supported Films of Poly (4-tert-butylstyrene). *ACS Macro Letters* **2017**, *6* (4), 354-358.

(35) Zhou, Y.; He, Q.; Zhang, F.; Yang, F.; Narayanan, S.; Yuan, G.; Dhinojwala, A.; Foster, M. D., Modifying Surface Fluctuations of Polymer Melt Films with Substrate Modification. *ACS Macro Letters* **2017**, *6* (9), 915-919.

(36) Akgun, B.; Uğur, G. k. e.; Jiang, Z.; Narayanan, S.; Song, S.; Lee, H.; Brittain, W. J.; Kim, H.; Sinha, S. K.; Foster, M. D., Surface dynamics of “dry” homopolymer brushes. *Macromolecules* **2009**, *42* (3), 737-741.

(37) Lee, J.; Akgun, B.; Jiang, Z.; Narayanan, S.; Foster, M., Altering surface fluctuations by blending tethered and untethered chains. *Soft Matter* **2017**, *13* (44), 8264-8270.

(38) Richardson, H.; Sferrazza, M.; Keddie, J., Influence of the glass transition on solvent loss from spin-cast glassy polymer thin films. *The European Physical Journal E* **2003**, *12* (1), 87-91.

(39) Cosgrove, T.; Crowley, T. L.; Ryan, K.; Webster, J. R., The effects of solvency on the structure of an adsorbed polymer layer and dispersion stability. *Colloids and Surfaces* **1990**, *51*, 255-269.

(40) Orts, W. J.; van Zanten, J. H.; Wu, W.-l.; Satija, S. K., Observation of temperature dependent thicknesses in ultrathin polystyrene films on silicon. *Physical Review Letters* **1993**, *71* (6), 867.

(41) Kanaya, T.; Miyazaki, T.; Watanabe, H.; Nishida, K.; Yamano, H.; Tasaki, S.; Bucknall, D., Annealing effects on thickness of polystyrene thin films as studied by neutron reflectivity. *Polymer* **2003**, *44* (14), 3769-3773.

(42) Binnig, G. K., Atomic force microscope and method for imaging surfaces with atomic resolution. Google Patents: 1988.

(43) Zhong, Q.; Inniss, D.; Kjoller, K.; Elings, V., Fractured polymer/silica fiber surface studied by tapping mode atomic force microscopy. *Surface Science Letters* **1993**, *290* (1-2), L688-L692.

(44) Gross, L.; Mohn, F.; Moll, N.; Liljeroth, P.; Meyer, G., The chemical structure of a molecule resolved by atomic force microscopy. *Science* **2009**, *325* (5944), 1110-1114.

(45) Kobayashi, S.; Inaba, K., X-ray thin-film measurement techniques. *Mass Spectroscopy Equipped with a Skimmer-type Interface* **2012**, *8*.

(46) Kiessig, H., Interference of X-rays in thick layers. *Ann Phys Berl* **1931**, *10* (7), 769-88.

(47) Bauer, B.; Fetters, L., Synthesis and dilute-solution behavior of model star-branched polymers. *Rubber Chemistry and Technology* **1978**, *51* (3), 406-436.

(48) He, Q. Synthesis of Cyclic and Multicyclic Polystyrenes and Their Surface Fluctuations in Melt Polymer Films. University of Akron, 2017.

(49) He, Q.; Mao, J.; Wesdemiotis, C.; Quirk, R. P.; Foster, M. D., Synthesis and Isomeric Characterization of Well-Defined 8-Shaped Polystyrene Using Anionic Polymerization, Silicon Chloride Linking Chemistry, and Metathesis Ring Closure. *Macromolecules* **2017**, *50* (15), 5779-5789.

(50) He, Q.; Yol, A. M.; Wang, S.-F.; Ma, H.; Guo, K.; Zhang, F.; Wesdemiotis, C.; Quirk, R. P.; Foster, M. D., Efficient synthesis of well-defined cyclic polystyrenes using anionic polymerization, silicon chloride linking chemistry and metathesis ring closure. *Polymer Chemistry* **2016**, *7* (37), 5840-5848.

(51) Ellison, C. J.; Mundra, M. K.; Torkelson, J. M., Impacts of polystyrene molecular weight and modification to the repeat unit structure on the glass transition— nanoconfinement effect and the cooperativity length scale. *Macromolecules* **2005**, *38* (5), 1767-1778.

(52) Qian, Z.; Minnikanti, V. S.; Sauer, B. B.; Dee, G. T.; Archer, L. A., Surface tension of symmetric star polymer melts. *Macromolecules* **2008**, *41* (13), 5007-5013.

(53) Piranha solution is dangerous, use with protection.

(54) Chremos, A.; Camp, P. J.; Glynos, E.; Koutsos, V., Adsorption of star polymers: computer simulations. *Soft Matter* **2010**, *6* (7), 1483-1493.

(55) Fetters, L.; Lohse, D.; Richter, D.; Witten, T.; Zirkel, A., Connection between polymer molecular weight, density, chain dimensions, and melt viscoelastic properties. *Macromolecules* **1994**, *27* (17), 4639-4647.

(56) Jenkins, F. A.; White, H. E., *Fundamentals of Optics*. Tata McGraw-Hill Education: 1937.

